

Orthogonally polarized self-mode-locked Nd:YAG laser with tunable beat frequencies

C. Y. Lee*, C. L. Sung, C. Y. Cho, H. P. Cheng, Y. F. Chen

Dept. of Electrophysics, National Chiao Tung Univ./ 1001 Ta-Hsueh Rd. Hsinchu, 30010 Taiwan

ABSTRACT

An orthogonally polarized self-mode-locked Nd:YAG laser is demonstrated in a short linear cavity. Under an incident pump power of 8.2 W, the average output power can be measured to be 3.8 W. The beat frequency Δf_c between two orthogonally polarized mode-locked components is observed and increases linearly with an increase in the incident pump power. The origin of the beat frequency is utterly confirmed to be caused by the thermal-stress-induced birefringence in the Nd:YAG crystal and is theoretically simulated. The present result provides a promising method to achieve orthogonally polarized mode-locked lasers with tunable beat frequency.

Keywords: Self-mode locking, orthogonal polarizations, Nd:YAG crystal, solid-state laser

1. INTRODUCTION

Orthogonally polarized dual-frequency laser sources are very attractive in many applications¹⁻³ and can be achieved by inserting some birefringence elements or inducing the birefringence in an isotropic medium, such as Nd:YAG crystal, for splitting the central frequencies of the orthogonal polarizations⁴⁻⁶. Recently, self-mode-locked (SML) operation, which means without any active or passive mode-locking elements except for the gain medium in the resonator, in Nd:YAG lasers has been reported. Therefore, it is of great interest to utilize Nd:YAG crystal as the gain medium for obtaining the orthogonally polarized SML output.

In this work, we thoroughly investigate the temporal dynamics of the polarization-resolved output intensity of a Nd:YAG laser with a short cavity. It is experimentally found that the SML operation can be realized in the two orthogonal polarizations along the principal axes simultaneously and then the central frequency difference between these two mode-locked components will lead to a beating in the polarization-resolved output intensity. The origin of the central frequency splitting is confirmed to be the thermal-induced birefringence in the Nd:YAG crystal. We believe the present finding can be developed as a promising approach for creating orthogonally polarized mode-locked lasers with tunable beat frequency.

2. EXPERIMENTAL SETUP

The schematic diagram of the experimental setup for the SML Nd:YAG laser is illustrated in Fig. 1(a). We used a plano-plano configuration to construct a short linear cavity with avoiding all unwanted reflection. The gain medium was an 1.0 at. % Nd:YAG rod with a length of 10 mm and a diameter of 4 mm. Both end surfaces of the laser rod were coated for anti-reflection (AR, $R < 0.2\%$) at 1064 nm. The gain crystal was wrapped with indium foil and slightly housed in a water-cooled copper holder with water temperature around 20 °C to ensure laser working stably. It is noteworthy that the side mount was used to reduce the weight of the copper holder acting on the crystal. A flat mirror whose entrance face was coated for AR at 808 nm and the second surface was coated for high-reflectance coating at 1064 nm ($R > 99.8\%$) together with high-transmission coating at 808 nm was exploited as the front mirror. The output coupler was a flat wedged mirror with a transmission of 18% at 1064 nm. The pump source was a random-polarized 10-W 808-nm fiber-coupled laser diode with a core diameter of 200 μm and a numerical aperture of 0.22. The pump beam was reimaged into the laser crystal with an average radius approximately 200 μm . The optical length of the laser cavity L_{opt} was set to be approximately 66~67mm.

*pomon.ep01g@nctu.edu.tw

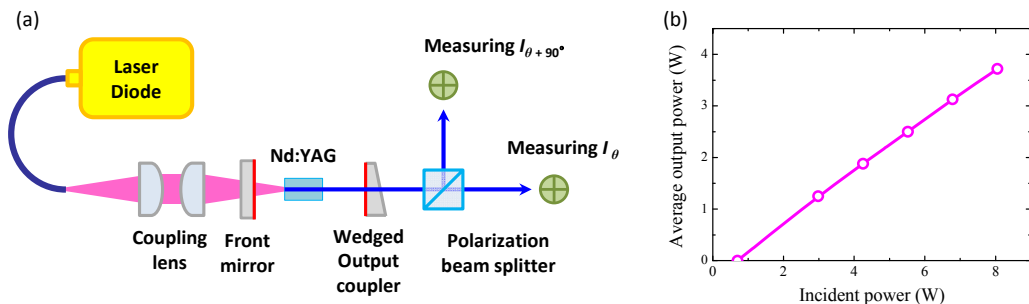


Figure 1. (a) Experimental setup. (b) Average output power with respect to the incident pump power.

3. EXPERIMENTAL RESULTS

To achieve a stable SML operation, the separation d between the Nd:YAG rod and the front mirror was set to be around 3 mm to reduce the spatial hole burning effect for limiting the lasing longitudinal mode number⁷. Experimental result of the average output power versus the incident pump power is demonstrated in Fig. 1(b). An average output power of 3.8 W was generated under an incident pump power of 8.2 W, corresponding to a slope efficiency of 50.7%.

The temporal behaviors of the laser total output were detected by a high-speed InGaAs photodetector, whose output signal was connected to a digital oscilloscope and to a RF spectrum analyzer. Figures 2(a) and 2(b) depict pulse trains on two different time scales at a 2.2-W pump power, one with 1- μ s time span for demonstrating the amplitude stability, and the other with 5-ns time span for demonstrating SML pulses. The power spectrum of the total output is shown in Fig. 2(c). As we can see that the peak values were generally greater than 45 dBm, indicating the well-behaved SML operation. The SML pulse width was measured by an autocorrelator as displayed in Fig. 2(d) and the FWHM was approximately 37 ps by assuming the Gaussian-shaped temporal profile.

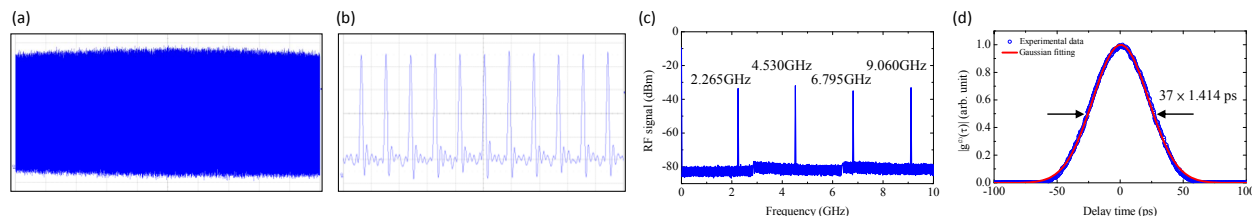


Figure 2. Pulse trains on two different time scales: (a) time span of 1 μ s; (b) time span of 5 ns; (c) RF power spectrum of the total output; (d) autocorrelation trace of the output pulses.

Next, the polarized behavior of the lasing output was studied and revealed that the lasing mode was composed of two orthogonally polarized eigenstates, which were defined to be along the x - and y -axes, with different central frequencies. The polarization-resolved output intensities $I_\theta(t)$ for $\theta = 0^\circ$, 90° , 45° , and 135° are demonstrated in Fig. 3(a)-3(d), respectively. Here, θ is the analyzer angle with respect to the x axis. As we can see that the pulse trains along the principal polarization directions are almost identical to the result of the total output intensity. Nevertheless, the pulse trains of the polarization-resolved intensities along 45° and 135° are observed to exhibit a phenomenon of intensity modulation. The beat frequency was further found to be increased linearly with an increase in the pump power, as shown in Figs. 4(a)-4(d) for $I_{45^\circ}(t)$ at four different pump powers. And experimental results for the beat frequency versus the pump power are shown in Fig. 5. In the following section, the beat frequency Δf_c is confirmed to result from the tiny birefringence induced by the thermal effect of the absorbed pump power in the Nd:YAG crystal⁸.

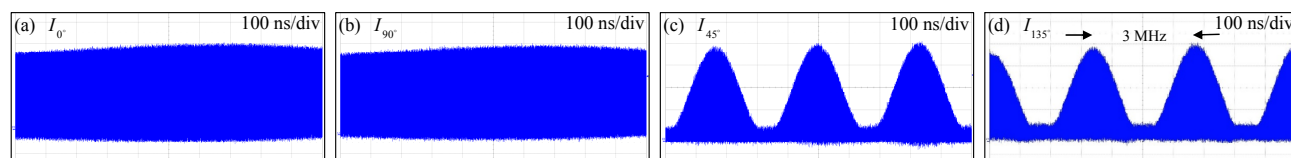


Figure 3. Temporal traces of polarization-resolved output intensities $I_\theta(t)$: (a) $\theta = 0^\circ$; (b) $\theta = 45^\circ$; (c) $\theta = 90^\circ$; (d) $\theta = 135^\circ$.

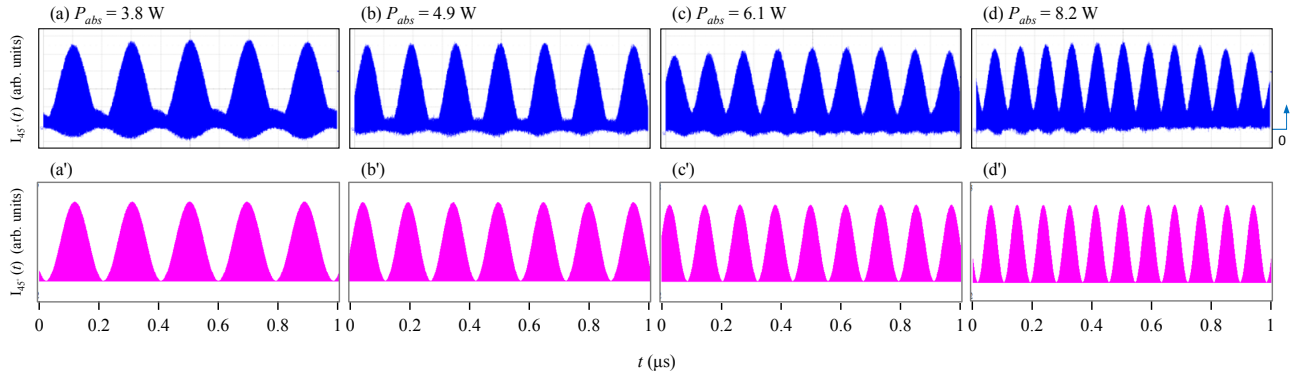


Figure 4. (a)-(d) Experimental data for $I_{45}(t)$ at four different pump powers; (a')-(d') theoretical simulations corresponding to data shown in (a)-(d), respectively.

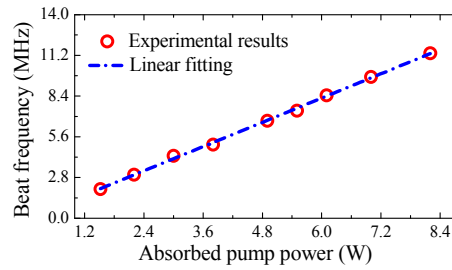


Figure 5. Beat frequency of the self-mode-locked Nd:YAG laser measured as a function of the absorbed pump power.

4. THEORETICAL SIMULATION

An optical isotropic material, such as YAG crystal becomes anisotropic while it is subject to mechanic stresses. The refractive index of a crystal is usually specified by the indicatrix, whose coefficients are the components of the relative dielectric impermeability tensor at optical frequencies⁹. Presuming the light propagates along the z axis, the mode-locked states formed by N longitudinal modes for the x - and y -polarizations can be expressed as

$$E_x(t) = E_{ox} \exp(-i2\pi f_{c,x}t) \frac{1}{N} \sum_{n=1}^N \exp \left[-i2\pi \left(n - \frac{N}{2} \right) f_{rep,x}t \right], \quad (1)$$

$$E_y(t) = E_{oy} \exp(-i2\pi f_{c,y}t) \frac{1}{N} \sum_{n=1}^N \exp \left[-i2\pi \left(n - \frac{N}{2} \right) f_{rep,y}t \right], \quad (2)$$

where E_{ox} and E_{oy} are the peak amplitudes, $f_{rep,x}$ and $f_{rep,y}$ are the round-trip frequencies, and $f_{c,x}$ and $f_{c,y}$ are the central frequencies for the x and y components, respectively.

Extending the analysis performed by Koechner and Rice⁸ to the end-pumped scheme¹⁰, the thermal-stress-induced birefringence can be given by

$$\Delta n = n_y - n_x = \frac{-\alpha_T \nu n_o^3 \xi P_{abs}}{24\pi(1-\nu)K_c L_{cry}} \frac{\omega_o^2(p_{11} - p_{12} + 4p_{44})}{\omega_p^2[1 + 2 \ln(r_o / \omega_p)]}, \quad (3)$$

where n_x and n_y are the refractive indices along the x and y axes, respectively, α_T is the linear expansion coefficient, K_c is the thermal conductivity, ν is the Poisson's ratio, p_{mn} are the elasto-optical coefficients, n_o is the refractive index without birefringence, ξ is the effective thermal loading, P_{abs} is the absorbed pump power in watts, r_o is the radius of the laser rod, is the length of the laser rod, ω_o is the radius of the cavity mode in the gain medium, and ω_p is the average radius of the pump beam. With the following parameters of $L_{cry} = 10$ mm, $r_o = 2.0$ mm, $\alpha_T = 7.9 \times 10^{-6}$ /°C, $K_c = 0.013$ W/mm°C, $\nu = 0.28$, $n_o = 1.82$, $p_{11} = -0.0290$, $p_{12} = 0.0091$, $p_{44} = -0.0615$, $\xi = 0.24$, $\omega_o = 215$ μ m, and $\omega_p = 200$ μ m, Δn can be calculated

to be $3.27 \times 10^{-8} P_{abs}$. This tiny birefringence will lead to a difference in the round-trip frequencies ($\Delta f_{rep} = f_{rep,y} - f_{rep,x} = f_{rep}(L_{cry}/L_{opt})\Delta n$) and in the central frequencies ($\Delta f_c = f_{c,y} - f_{c,x} = f_c(L_{cry}/L_{opt})\Delta n$) between two orthogonally polarized pulse trains. Here $f_{rep} = c/2L_{opt}$ is the round-trip frequency without birefringence, f_c is the frequency of the gain peak, and $L_{opt} = L_{cav} + (n_o - 1)L_{cry}$, where L_{cav} is the geometric length of the cavity. Using $f_{rep} = 2.265$ GHz, $f_c = 281.85$ THz, $L_{opt} = 66.2$ mm, and $\Delta n = 3.27 \times 10^{-8} P_{abs}$, Δf_{rep} and Δf_c can be found to be $11.19P_{abs}$ Hz and $1.39P_{abs}$ MHz, respectively. For the pump power P_{abs} in a range of 1-10 W, we can find that Δf_{rep} varies only from a few to several tenths hertz, indicating two orthogonally polarized pulse trains are nearly synchronous. However, Δf_c will be approximately in the range of 1-15 MHz for the pump power P_{abs} within 1-10 W, which cannot be neglected. Note the analyzed result of $\Delta f_c = 1.39P_{abs}$ MHz is consistent with the experimental result shown in Fig. 5.

Substituting $f_{rep,x} = f_{rep,y} = f_{rep}$ and $E_{ox} = E_{oy} = E_o$ into Eqs. (1) and (2) and using $\Delta f_c = f_{c,y} - f_{c,x}$, the polarization-resolved output intensity can be given by

$$I_{\theta}(t) = \left| E_o \frac{\sin(\pi N f_{rep} t)}{N \sin(\pi f_{rep} t)} \right|^2 [1 + \sin(2\theta) \cos(2\pi \Delta f_c t)]. \quad (4)$$

For $N = 5$ and the above-mentioned parameters, $I_{\theta}(t)$ can be numerically calculated. Calculated results for $I_{45^{\circ}}(t)$ at four pump powers are depicted in Fig. 4(a')-4(d') and agree very well with experimental data for all cases shown in Fig. 4(a)-4(d), respectively. This excellent agreement not only confirms that the beat frequency Δf_c comes from the thermally induced birefringence but also validates the present analysis.

5. CONCLUSION

In conclusion, we have employed a linear cavity to achieve the simultaneous self-mode-locking of two orthogonally polarized states in a Nd:YAG laser. An average output power of 3.8 W could be obtained at an incident pump power of 8.2 W. The beat frequency Δf_c between two orthogonally polarized mode-locked components have been observed and measured precisely. Experimental observations for the beating between two orthogonally polarized mode-locked components can be thoroughly elucidated by considering the thermally induced birefringence in the Nd:YAG crystal. This work is expected to offer a promising method for generating orthogonally polarized mode-locked lasers with tunable beat frequency.

REFERENCES

- [1] J. T. Kringlebotn, W. H. Loh, and R. I. Laming, "Polarimetric Er³⁺-doped fiber distributed-feedback laser sensor for differential pressure and force measurements," Opt. Lett. 21(22), 1869-1871 (1996).
- [2] W. Holzappel and U. Riss, "Computer-based high resolution transmission ellipsometry," Appl. Opt. 26(1), 145-153 (1987).
- [3] D. Liu, N. Q. Ngo, X. Y. Dong, S. C. Tjin, and P. Shum, "A stable dual-wavelength fiber laser with tunable wavelength spacing using a polarization-maintaining linear cavity," Appl. Phys. B 81(6), 807-811 (2005).
- [4] S. L. Zhang and W. Holzappel, [Orthogonal Polarization in Lasers: Physical Phenomena and Engineering Applications], Wiley (2013).
- [5] S. Yang, and S. L. Chang, "The frequency split phenomenon in a He-Ne laser with a rotational quartz plate in its cavity," Opt. Commun. 68(1), 55-57 (1988).
- [6] S. L. Chang, M. Lu, and M. X. Wu, "Laser frequency split by an electro-optical element in its cavity," Opt. Commun. 96(4), 245-248 (1993).
- [7] Y. F. Chen, Y. J. Huang, P. Y. Chiang, Y. C. Lin, and H.C. Liang, "Controlling number of lasing modes for designing short-cavity self-mode-locked Nd-doped vanadate lasers," Appl. Phys. B 103(4), 841-846 (2011).
- [8] W. Koechner and D. K. Rice, "Effect of Birefringence on the performance of linearly polarized YAG:Nd lasers," IEEE J. Quantum Electron. 6(9), 557-566 (1970).
- [9] J. F. Nye, [Physical Properties of Crystals], Oxford University Press, London (1964).
- [10] Y. F. Chen, T. M. Huang, C. F. Kao, C. L. Wang, and S. C. Wang, "Optimization in scaling fiber-coupled laser-diode end-pumped lasers to higher power: influence of thermal effect," IEEE J. Quantum Electron. 33(8), 1424-1429 (1997).